



RVE-BASED MICROMECHANICAL ANALYSIS OF FIBER-MATRIX DEBONDING IN THIN PLY FRPC LAMINATES

FINITE ELEMENT MODEL: GEOMETRY AND DISCRETIZATION
L. Di Stasio^{1,2}, Z. Ayadi¹, J. Varna²

¹ EEIGM, Université de Lorraine, Nancy, France ² Division of Materials Science, Luleå University of Technology, Luleå, Sweden









Outline

- The kinks in thin ply mechanics
- Geometries
- Body-fitted grids for the simulation of fracture propagation in curved domains
- Appendices









જ) વ (3

Thin ply mechanics Geometries Body-fitted grids Appendices

Work-flow of composite structural design Failure load analysis Progressive load analysis

THIN PLY MECHANICS









Work-flow of composite structural design

Work-flow of composite structural design Failure load analysis Progressive load analysis









Work-flow of composite structural design Failure load analysis Progressive load analysis

Failure load analysis









Work-flow of composite structural design Failure load analysis Progressive load analysis

Progressive load analysis









■ GEOMETRIES

RVE-BASED MICROMECHANICAL ANALYSIS OF FIBER-MATRIX DEBONDING IN THIN PLY FRPC LAMINATES

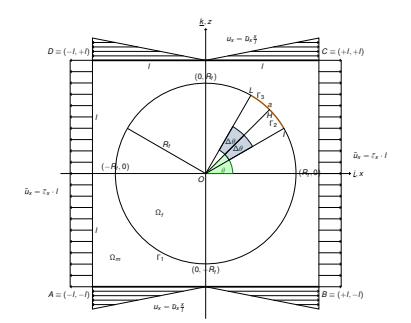


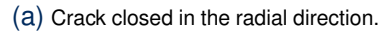
L. Di Stasio1,2, Z. Ayadi1, J. Varna2

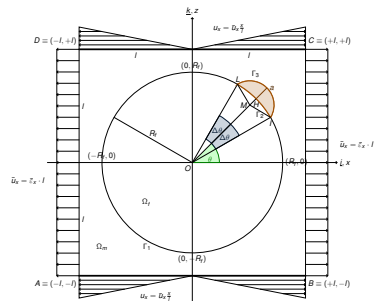


Geometries Body-fitted grids

Single RVE model







(b) Crack open in the radial direction.



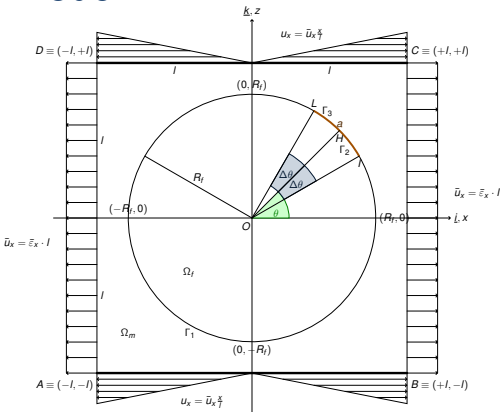






Geometries Body-fitted grids **Appendices**

Single RVE model



Initial state of single RVE model: crack closed in the radial direction.





 $K = (-I, +t_{ratio} \cdot I)$

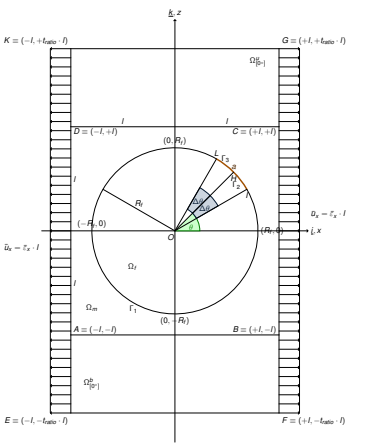


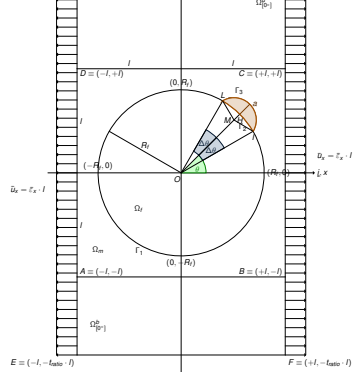
 $G = (+I, +t_{ratio} \cdot I)$



Geometries Body-fitted grids Appendices

Bounded RVE model





(a) Crack closed in the radial direction.

(b) Crack open in the radial direction.





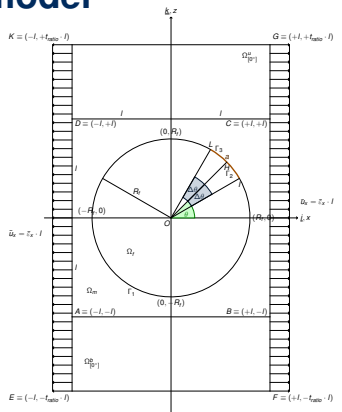




chanics Geometries Body-fitted grids

Appendices

Bounded RVE model



Initial state of bounded RVE model: crack closed in the radial direction.



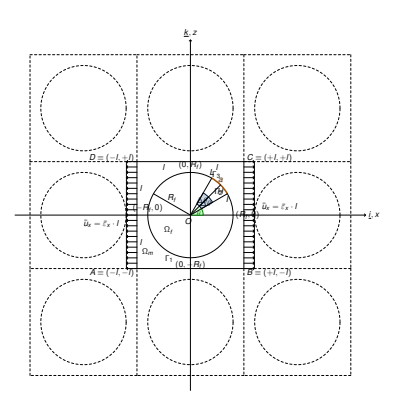


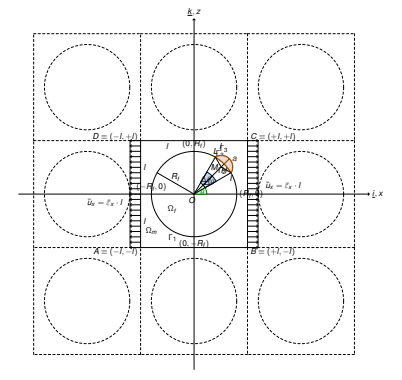






Periodic RVE model





(a) Crack closed in the radial direction.

(b) Crack open in the radial direction.





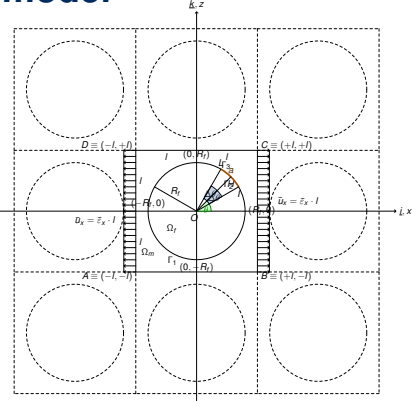




Geometries Body-fitted grids

Appendices

Periodic RVE model



Initial state of periodic RVE model: crack closed in the radial direction.











Summary of designed geometries

Name

Number of phases

single-RVE

į

Description

Circular fiber inside a square matrix domain.

Geometry of each phase

Fiber: circular; matrix: square with circular inclusion at its center.

Boundary conditions

Constant strain at $z = \pm I$; in order to have constant strain, the displacement has a linear functional form, i.e. $u_x|_{z=\pm I} = \bar{u}_x \frac{x}{I}$.

Imposed conditions

Constant displacement $u_x|_{z=\pm l} = \bar{u}_x = \bar{\varepsilon}_x \cdot l$ at $x = \pm l$.











Geometries Body-fitted grids Appendices

Summary of designed geometries

Name bounded-RVE **Number of phases**

- 3

Description

Circular fiber inside a square matrix domain, bounded by two UD rectangular domains on the upper and lower side.

Geometry of each phase

Fiber: circular; matrix: square with circular inclusion at its center; UD: rectangular.

Boundary conditions

Free surface at $z = \pm I$.

Imposed conditions

Constant displacement $u_x|_{z=\pm l} = \bar{u}_x = \bar{\varepsilon}_x \cdot l$ at $x = \pm l$.







Geometries Body-fitted grids Appendi

Summary of designed geometries

Name

Number of phases

periodic-RVE

2

Description

Periodically repeated unit cell, constituted by a circular fiber inside a square matrix domain.

Geometry of each phase

Fiber: circular; matrix: square with circular inclusion at its center.

Boundary conditions

Periodic boundary conditions on all sides.

Imposed conditions

Constant displacement $u_x|_{z=\pm l} = \bar{u}_x = \bar{\varepsilon}_x \cdot l$ at $x = \pm l$.











かなぐ 17

Thin ply mechanics Geometries Body-fitted grids Appendices
Introduction Mesh generation algorithms Differential geometry algorithms

■ BODY-FITTED GRIDS









The issues

- Mesh characteristics (elements' size and distribution, irregularities) affect the behaviour of numerical models used to simulate fracture propagation
- The presence of curved boundaries induce irregularities in the mesh, using quadrilaterals as well as triangular elements









The issues

- Abaqus softwares' package provides powerful algorithms for the Finite Elements Method (global to local node mapping, application of load and boundary conditions, solvers)
- On the other hand, the meshing capabilities offered by Abaqus are restricted
 - Using Abaqus/CAE, mesh parameterization is not possible and the meshing process is controlled only through a few parameters, no access to the algorithms is provided
 - Abaqus Python scripting grants some degree of parameterization, but it allows the automation of CAE commands; thus, there is no direct access to the meshing algorithms
 - Abaqus input file scripting provides greater access to the meshing algorithms and allows for parameterization of simple geometries; complex arrangements are much more difficult, or even impossible, to parameterize using this kind of scripting









The issues

- Tools for the analysis and control of the mesh are limited in Abaqus
- No field variable is provided to measure the quality of the mesh









The objectives

- Develop a toolbox of algorithms to:
 - Develop a toolbox of algorithms to:
 - 2. generate meshes of curvilinear domains in 2D and 3D
 - 3. provide control of the mesh down to the single node/element
 - 4. allow for efficient parameterization of the grid generation process
 - 5. provide quantitative tools for the analysis of mesh quality properties

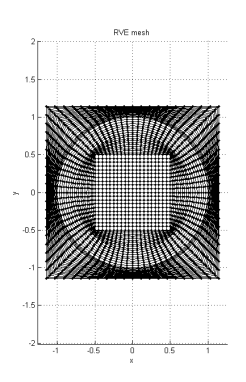








The result









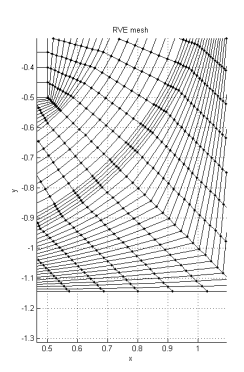


୬) Q (∿ 23

Thin ply mechanics Geometries Body-fitted grids Appendices Introduction Mesh generation algorithms Differential geometry algorithms

The result

L. Di Stasio1,2, Z. Ayadi1, J. Varna2







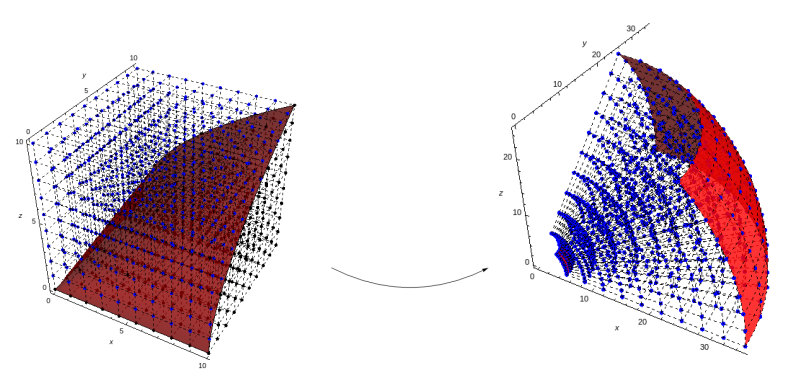




Geometries Body-fitted grids Appendices Thin ply mechanics Mesh generation algorithms Differential geometry algorithms Introduction

Fundamental ideas

One-to-one mapping



Computational domain

Physical domain





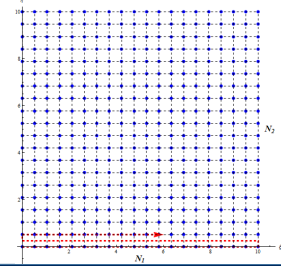


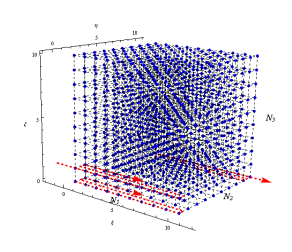


Fundamental ideas

Helical numbering

- **N**₁, N_2 , N_3 number of grid points respectively along ξ -, η -, ζ direction in computational space
- Total number of points $N = N_1 \cdot N_2$ in 2D and $N = N_1 \cdot N_2 \cdot N_3$ in 3D
- Helical numbering: given $n \in [1, N]$, $i \in [1, N_1]$, $j \in [1, N_2]$, $k \in [1, N_3]$, $n = i + (j 1) \cdot N_1$ in 2D and $n = i + (j 1) \cdot N_1 + (k 1) \cdot N_1 \cdot N_2$ in 3D











Mesh generation

Numerical strategy for structured grid generation in curved geometries - 3D

- 1. The boundary is generated patching analytical parameterizations
- 2. The boundary is split into a set of 8 corners (c_i) , 12 edges (e_i) , 4 surfaces (f_i)
- Interior nodes are created applying transfinite interpolation using multi-dimensional linear Lagrangian or Hermite interpolants

$$P_1(x, p_j) = \sum_{j=1}^n p_j \prod_{k=1, k \neq j}^n \frac{x - x_k}{x_j - x_k}$$

$$\begin{split} P_2(x,y,p_j,q_j) &= P_1(x,p_j) \otimes P_1(y,q_j) &\quad P_3(x,y,z,p_j,q_j,r_j) = P_1(x,p_j) \otimes P_1(y,q_j) \otimes P_1(z,r_j) \\ r_i(\xi,\eta,\zeta) &= P_1(\xi,f_5,f_3) + P_1(\eta,f_2,f_4) + P_1(\zeta,f_1,f_6) - P_2(\xi,\eta,c_1,c_2,c_3,c_4) + \\ &\quad - P_2(\xi,\eta,e_5,e_6,e_7,e_8) - P_2(\xi,\zeta,e_2,e_4,e_{10},e_{12}) - P_2(\eta,\zeta,e_1,e_3,e_9,e_{11}) + \\ &\quad + P_3(\xi,\eta,\zeta,c_1,c_2,o_3,c_4,c_5,e_6,c_7,e_8) \end{split}$$

4. The mesh is smoothed applying elliptic mesh generation

$$g^{11}\underline{r}_{,\xi\xi}+2g^{12}\underline{r}_{,\xi\eta}+g^{22}\underline{r}_{,\eta\eta}+2g^{13}\underline{r}_{,\xi\zeta}+g^{33}\underline{r}_{,\zeta\zeta}+2g^{23}\underline{r}_{,\eta\zeta}=0$$

RVE-BASED MICROMECHANICAL ANALYSIS OF FIBER-MATRIX DEBONDING A \bullet \bullet \bullet \bullet









Geometries Body-fitted grids Appendices Mesh generation algorithms Differential geometry algorithms

Mesh generation

Numerical strategy for structured grid generation in curved geometries (More)



- For both transfinite interpolation and elliptic mesh generation, Dirichlet boundary conditions are assigned, i.e. boundaries are fixed
- Elliptic mesh generation is solved iteratively: at step *n*, the contravariant metric components are computed based on configuration at step n-1 and afterwards the configuration is updated
- Partial differential equations are discretized using second order central finite difference scheme for second derivatives:

$$\frac{\partial^2 u}{\partial (q^i)^2}|_{q^i} = \frac{u_{i+1} - 2u_i + u_{i-1}}{(\Delta q^i)^2} - \frac{(\Delta q^i)^2}{12} \frac{\partial^4 u}{\partial (q^i)^4}|_{q^i} + \dots$$

An algebraic system of equations $\underline{Ax} = \underline{b}$ is obtained; it is solved using built-in libraries in Matlab, and implementing an iterative Jacobian-Free Newton-Krylov (JFNK) method in C++

Management of boundaries is done exclusively using indices, not using coordinates: indices of nodes on corners, edges, faces are stored at the beginning of computation RVE-BASED MICROMECHANICAL ANALYSIS OF FIBER-MATRIX DEBONDING THIN PLY FRPC LAMINATES



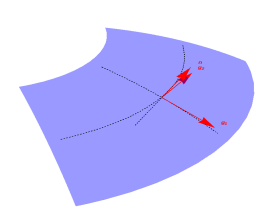


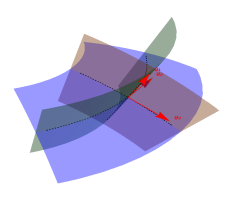




Differential geometry

Computation of geometric properties of mappings





- Given analytical parameterization, using symbolic computing (Mathematica)
- Given discrete data, using numerical computing (Matlab, C++)
 - For 2D and 3D geometries, surfaces in 3D space







Differential geometry

$$\underline{R} = r_i = r_i(q^i)$$
 $\underline{g}_i = \frac{\partial \underline{R}}{\partial q^i}$
 $\underline{g}_3 = \underline{g}_1 \times \underline{g}_2$ for surfaces
 $g_{ij} = \underline{g}_i \cdot \underline{g}_j$
 $g = \det(g_{ij})$
 $\underline{g}^i = \frac{\underline{g}_j \times \underline{g}_k}{\sqrt{g}}$
 $g^{ij} = \underline{g}^i \cdot \underline{g}^j$
 $v_i = \underline{v} \cdot g_i$ $v^i = \underline{v} \cdot g^i$

$$\underline{v} = \sum_{i} v_{i} \underline{g}^{i} \quad \underline{v} = \sum_{i} v^{i} \underline{g}_{i}$$

$$[ij, k] = \underline{g}_{i,j} \cdot \underline{g}_{k}$$

$$\Gamma_{ij}^{k} = \underline{g}_{i,j} \cdot \underline{g}^{k}$$

$$R_{ijk}^{l} = \Gamma_{ik,j}^{l} - \Gamma_{ij,k}^{l} + \Gamma_{ls}^{l} \Gamma_{ik}^{s} - \Gamma_{ks}^{l} \Gamma_{ij}^{s}$$

$$R_{iklm} = g_{ls} R_{ijk}^{s}$$

$$R_{ij} = g^{lm} R_{iljm}$$

$$R = g^{ij} R_{ij}$$







Differential geometry



First derivatives computed with second order finite differences

$$\frac{\partial u}{\partial q^i}|_{q^i} = \frac{u_{i+1} - u_{i-1}}{2\Delta q^i} - \frac{(\Delta q^i)^2}{6} \frac{\partial^3 u}{\partial (q^i)^3}|_{q^i} + \dots$$

Right- and left- sided second order finite differences at boundary

$$\frac{\partial u}{\partial q^i}|_{q^i} = \frac{-3u_i + 4u_{i+1} - u_{i+2}}{2\Delta q^i} + \frac{(\Delta q^i)^2}{3} \frac{\partial^3 u}{\partial (q^i)^3}|_{q^i} + \dots$$

$$\frac{\partial u}{\partial q^i}|_{q^i} = \frac{3u_i - 4u_{i-1} + u_{i-2}}{2\Delta q^i} + \frac{(\Delta q^i)^2}{3} \frac{\partial^3 u}{\partial (q^i)^3}|_{q^i} + \dots$$

 Δq^i are assumed to be constant in space and time but could be different between different directions, as considered in the computational space



Additional details







THANK YOU!









Geometries Body-fitted grids **Appendices**

APPENDICES

RVE-BASED MICROMECHANICAL ANALYSIS OF FIBER-MATRIX DEBONDING IN THIN PLY FRPC LAMINATES









Geometries Body-fitted grids

, iiiida giida ,

Differential geometry

Details on Matlab implementation

- In array firstdevneighbours of dimension N × 4D, neighbours and type of finite difference scheme (encoded with an integer mask, from 1 to 3) are stored for each grid site
- Each geometric quantity is stored in array of dimension N × Dⁿindices; i.e. tensor components are stored in columns N × 1 stacked together in a single global array
- Symmetry of geometric quantities (for example, $g_{ij} = g_{ji}$) is exploited: components that can be recovered by symmetry are not saved to disk

Back to Differential geometry







Geometries

Body-fitted grids



Differential geometry

Details on C++ implementation

Back to Differential geometry

RVE-BASED MICROMECHANICAL ANALYSIS OF FIBER-MATRIX DEBONDING IN THIN PLY FRPC LAMINATES











Mesh generation

Numerical strategy for structured grid generation in curved geometries - 2D

- 1. The boundary is generated patching analytical parameterizations
- 2. The boundary is split into a set of 4 corners (c_i) and 4 edges (e_i)
- Interior nodes are created applying transfinite interpolation using multi-dimensional linear Lagrangian interpolants

$$P_1(x,p_j) = \sum_{j=1}^n p_j \prod_{k=1}^n \frac{x - x_k}{x_j - x_k} \quad P_2(x,y,p_j,q_j) = P_1(x,p_j) \otimes P_1(y,q_j)$$

$$r(\xi, \eta) = P_1(\xi, e_2, e_4) + P_1(\eta, e_1, e_3) - P_2(\xi, \eta, c_1, c_2, c_3, c_4)$$

4. The mesh is smoothed applying elliptic mesh generation

$$g^{11}\underline{r}_{,\xi\xi} + 2g^{12}\underline{r}_{,\xi\eta} + g^{22}\underline{r}_{,\eta\eta} = 0$$

Back to Mesh generation









Geometries Body-fitted grids Appendices

T P

Geometry and mesh generation

Numerical strategy for monolithic domains

- Cells are indexed with the same criteria applied to nodes and can be accessed using look-up tables of such indices
- 3D geometries can be costructed directly using 3D transfinite interpolation and 3D elliptic smoothing or can be generated as extrusion of 2D geometries
- If needed, cells can be accessed and modified, i.e. creating triangles/tetrahedra instead of squares/cubes

Back to Mesh generation











Geometries Body-fitted grids

Appendice

Geometry and mesh generation

Numerical strategy for domains with random inclusions

- 2D and 3D Ising model is applied to generate a porous geometry, controlling the dimensions of structures through the 'temperature' of the sytem
- Nodes with positive magnetization are assigned to one material domain and those negative to the other material (or viceversa)
- Boundaries of the 2 domains are identified checking magnetization of neighbours
- Both domains are then separately smoothed using elliptic mesh generation iterations

Back to Mesh generation



